REPORT DOCUMENTATION PAGE

Form Approved
OMB No. 0704-0188

1. REPORT DATE *(DD-MM-YYYY)*	**2. REPORT TYPE**	**3. DATES COVERED** *(From - To)*
17-07-2008	Journal Article	

4. TITLE AND SUBTITLE

Resonant Laser Ignition Study of Han-Hehn Propellant Mixture (Preprint)

5a. CONTRACT NUMBER

5b. GRANT NUMBER

5c. PROGRAM ELEMENT NUMBER

6. AUTHOR(S)
Angelo J. Alfano (Northrop Grumman Space Technology); Jeffrey D. Mills & Ghanshyam L. Vaghjiani (AFRL/RZSP)

5d. PROJECT NUMBER

5e. TASK NUMBER

5f. WORK UNIT NUMBER
23030423

7. PERFORMING ORGANIZATION NAME(S) AND ADDRESS(ES)

Air Force Research Laboratory (AFMC)
AFRL/RZSP
10 E. Saturn Blvd.
Edwards AFB CA 93524-7680

8. PERFORMING ORGANIZATION REPORT NUMBER

AFRL-RZ-ED-JA-2008-333

9. SPONSORING / MONITORING AGENCY NAME(S) AND ADDRESS(ES)

Air Force Research Laboratory (AFMC)
AFRL/RZS
5 Pollux Drive
Edwards AFB CA 93524-7048

10. SPONSOR/MONITOR'S ACRONYM(S)

11. SPONSOR/MONITOR'S NUMBER(S)
AFRL-RZ-ED-JA-2008-333

12. DISTRIBUTION / AVAILABILITY STATEMENT

Approved for public release; distribution unlimited (PA #08318A).

13. SUPPLEMENTARY NOTES
For publication in Combustion Science & Technology.

14. ABSTRACT

Resonant laser ignition at wavelengths in the UV and IR was demonstrated for hydroxyl ammonium nitrate (HAN) – hydroxyethylhydrazinium nitrate (HEHN) mixtures. This prototypical ionic liquid propellant was successfully and reliably ignited/detonated under confinement with single laser pulses in the mid IR at 2.94 and 10.6 μm. UV wavelengths at 193 and 248 nm were also resonant with sample absorption but they did not lead to ignition with the available excimer laser pulse energies. The results are consistent with absorption of the IR laser pulse within a short path, efficient V→T relaxation, and thermal decomposition of HAN that leads to additional chemical reaction and ignition/detonation of milligram samples within tens of microseconds.

15. SUBJECT TERMS

16. SECURITY CLASSIFICATION OF:			**17. LIMITATION OF ABSTRACT**	**18. NUMBER OF PAGES**	**19a. NAME OF RESPONSIBLE PERSON**
					Dr. Jeffrey Mills
a. REPORT	**b. ABSTRACT**	**c. THIS PAGE**	SAR	26	**19b. TELEPHONE NUMBER** *(include area code)*
Unclassified	**Unclassified**	**Unclassified**			N/A

Standard Form 298 (Rev. 8-98)
Prescribed by ANSI Std. 239.18

Resonant Laser Ignition Study of HAN-HEHN Propellant Mixture (Preprint)

Angelo J. Alfano *
Northrop Grumman Space Technology
One Space Park M5/1085
Redondo Beach, CA 90278

Jeffrey D. Mills and Ghanshyam L. Vaghjiani*
Propellants Branch, Space and Missile Propulsion Directorate
AFRL/RZSP
10 E. Saturn Blvd.
Edwards AFB, CA 93524

Abstract

Resonant laser ignition at wavelengths in the UV and IR was demonstrated for hydroxyl ammonium nitrate (HAN) - hydroxyethylhydrazinium nitrate (HEHN) mixtures. This prototypical ionic liquid propellant was successfully and reliably ignited/detonated under confinement with single laser pulses in the mid IR at 2.94 and 10.6 μm. UV wavelengths at 193 and 248 nm were also resonant with sample absorption but they did not lead to ignition with the available excimer laser pulse energies. The results are consistent with absorption of the IR laser pulse within a short path length, efficient V→ T relaxation, and thermal decomposition of HAN that leads to additional chemical reaction and ignition/detonation of milligram samples within tens of microseconds.

* Corresponding Authors; Email: angelo.alfano@ngc.com

ghanshyam.vaghjiani@edwards.af.mil

Keywords: laser ignition, ionic liquid propellant

Introduction

A large body of published research exists for ignition and combustion studies of substituted ammonium nitrate derivatives formulated as liquids with fuel and oxidizer partners [1-10]. The hydroxylammonium nitrate (oxidizer) and triethanol ammonium nitrate (fuel), HAN-TEAN, mixture is a prominent example that was investigated for liquid gun propellant applications. Laser ignition studies were predominantly nonresonant at 694 nm (ruby laser) [3] and 1.05 μm (Nd glass laser) [5,6] and multijoule pulse energies were involved. Carbon dioxide and pulsed excimer lasers were also applied [5,8]. Attempts to study the single drop[2,4] as well as bulk [6,7,9] sample combustion properties of these materials were reported along with informative thermogravimetric results[10,11]. Several conclusions were derived from this work:

a) Samples that contained significant amounts of water did not begin thermal decomposition until sufficient sustained energy to drive off the water was provided.

b) Exothermic thermal decomposition of HAN at 165 C was the initial reaction.

c) Pressurizing the sample lowered the laser ignition energy threshold for pulsed, nonresonant laser experiments.

d) Unconfined droplets were typically shattered and not completely ignited by thermal or optical energy.

The HAN-HEHN mixture includes both substituted ammonium nitrate as well as substituted hydrazinium nitrate constituents. The presence of the N-N bond stretch in HEHN provides a strong absorption resonance with the CO_2 laser

wavelength that was not present in previous laser ignition studies of ammonium nitrate derivative mixtures. This N-N stretching resonance at 10.6 μm as well as overlapping N-H and O-H resonances at 2.94 μm (Er-YAG laser) provide a system where multiple infrared (IR) resonant ignition wavelengths can be tested. This molecular framework also provides ultraviolet (UV) absorption resonance with the excimer laser at 193 and 248 nm.

The low vapor pressure of ionic liquid (IL) based propellants is a challenge with respect to ignition. However, a homogeneous single phase sample composition and the use of a single pulse, resonant monochromatic laser source is a well controlled environment for an ignition study. The experiments are much more reliably connected to a unique photophysical event, an ensuing chemical reaction mechanism, and subsequent ignition/detonation behavior. Analogous optical ignition studies from the UV to the IR on complex solid compositions[12-14] highlight the advantage of our approach to the study of IL ignition behavior. This paper summarizes the application of single resonant IR and UV laser pulses with respect to microliter HAN-HEHN-water sample ignition under confinement. The infrared results are adequately interpreted in terms of a simple vibrational to translational (V→ T) relaxation that creates a T-jump capable of initiating a reaction chain that begins with HAN thermal decomposition. Positive results at two IR wavelengths suggest that any mid IR laser source that couples to a strong absorption band in a HAN-fuel blend could also provide single pulse ignition/detonation. The laser power density and spot size needed to extend these results to larger samples can be predicted by the adaptation of modeling

formalism previously reported for solid propellant laser ignition [15-17]. The inclusion of a chemical heat release term in the form of an Arrhenius expression within a heat conduction model can also give valuable insight into the rate limiting ignition reaction chemistry. Such an extension of this study is in progress.

Experimental

The IL sample composition used in this study contained hydroxyl ammonium nitrate (HAN), hydroxyethylhydrazinium nitrate (HEHN), and only residual H_2O plus insignificant amounts of additional additives. Similar HAN-HEHN formulations have been studied with respect to ease of preparation, safe handling, and combustion properties[18]. *CAUTION*: The experimental results obtained in this paper were on sample sizes of tens of milligrams. The energy release from these confined sample sizes requires strict adherence to safety precautions that include hearing and blast protection near the experiment as well as adequate venting of the reaction products.

The UV absorption spectrum of the HAN-HEHN mixture that was highly diluted with water is shown in Figure 1. The positions of the excimer laser wavelengths at 193 (ArF) and 248 (KrF) nm are highlighted and an expanded view revealed an appreciable absorption on the long wavelength tail of the main feature at 248 nm (Figure 1, inset).

The mid IR absorption spectrum of a thin film of the IL mixture was taken between 2 mm thick BaF_2 windows. The Er-YAG laser emits at 2.94 microns where overlapping resonances from N-H and O-H vibrational stretching modes of HAN and HEHN appear in Figure 2. The N-N vibrational stretch in HEHN is

responsible for an overlap with the P_{20} line of the CO_2 laser at 10.6 μm in Figure 2. The vibrational frequency of the N-N stretch with the nitrogen atoms bound to hydrogen appears at higher wavenumbers but it is red-shifted toward 943 cm^{-1} when hydrogen is replaced with heavier substituents [19].

The CO_2 laser source was a pulsed TEA model that was capable of producing 2 joules per pulse without single rovibrational line selection at a maximum repetition rate of 5Hz. A time-resolved FTIR spectrum (5 ns per slice) of the laser output in Figure 3 indicates that the pulse is spread over several lines between 925 and 950 cm^{-1} during the first 50 ns and then the P_{20} transition at 943 cm^{-1} dominates. The broad sample absorption feature near 10.6 μm in Figure 2 is well matched to the various CO_2 laser lines. The temporal envelope of the pulse was detected with a room temperature, HgCdZnTe photovoltaic detector that had a < 1 ns response time and a sensitivity range from 2-12 μm. Figure 4 b reveals the characteristic early spike of the CO_2 TEA laser followed by a slowly decaying tail that extends to 1.3 μs. A single pulse from the free running laser at <1 Hz was selected for the ignition experiments by manually removing a graphite beam stop. The central portion of the rectangular beam passed through a 3/4 inch diameter circular graphite aperture and a 1 meter focal length NaCl lens. An additional aperture was used to reduce the laser spot size to less than the sample diameter. The energy within the laser pulse had a measured uniform top hat distribution across the beam.

The Er-YAG laser was constructed in a compact breadboard format. The pulse profile of the 2.94 μm output appears in Figure 4 c. Considerable spiking is evident on a single shot basis. The pulse energy, rep rate, and pulse duration were variable and a 232 μs FWHM pulse in the 400 to 600 mJ range was mechanically selected from the free running laser at 2 Hz. A top hat energy distribution was exhibited.

An excimer laser was used to provide 13 ns pulses (Figure 4 a) at 193 nm (115 mJ) and 248 nm (250 mJ). An argon, fluorine, and helium mixture provided the ArF excimer emission at 193 nm. A krypton, fluorine, and helium mixture produced 248 nm emission from the KrF excimer. An avalanche photodiode with a 200 ps rise time was used to measure the temporal profile of a low energy surface reflection from the laser pulse.

A variety of sample cell geometries was explored with volumes of 66, 31, 19, and 11 μl in Figure 5 a through d, respectively. The cell material was 316 stainless steel and in all cases the sample was confined in a top hat or cylindrical well that was “O” ring sealed with a 2 mm thick IR transmitting window (BaF_2, CaF_2, or ZnSe). S1-UV grade fused silica windows from 1/16 to 3/16 inch thickness were used with the excimer laser. Another “O” ring was then placed over the outer surface of the window and a cover plate with a circular aperture was bolted to the cell face to secure the window. A cell design that included a fast response pressure transducer was similar to that in Figure 5 a. The pressure transducer was threaded through the rear of the cell and the circular transducer face served as the bottom of the sample well. A brass “O” ring on the transducer body sealed

the transducer against a counter bore in the rear surface of the cell. The pressure transducer face had an invar membrane that was covered with a piece of polyester tape to minimize the metal to sample contact area. The transducer had a 20,000 psi maximum static rating, a <1 microsecond rise time, and a 500 kHz resonant frequency. Experiments that did not involve the pressure transducer also included a layer of tape at the base of the sample well.

Results and Discussion

Carbon Dioxide Laser Experiments

Figure 6 displays the results for ignition/detonation events that were obtained on a 66 µl sample that was contained in a cell dimensioned as in Figure 5 a. A single, multiline CO_2 laser pulse of 597 mJ at 10.6 µm was used and a portion of the laser pulse that was reflected from a graphite aperture was used to trigger the digital oscilloscope to generate the trace in Figure 6. In Figure 6a a photodiode that had a broad response across the visible and near IR was positioned near the sample cell and behind a Plexiglas shield to register the optical emission from the sample. A pressure transducer was placed 3 cm from the cell and it recorded the passage of the gases that were expelled during the ensuing ignition/detonation. The optical emission rises without delay after the laser pulse and decays after the reacting sample destroys the cell window. For Figure 6b the cell included a calibrated pressure transducer whose front face served as the base of the sample well. The pressure rise is delayed by 5 microseconds but the self pressurization within the sample cell exceeds the rating of the transducer leading to its destruction and that of the 2mm thick BaF_2

window within 30 μs of the laser pulse. The small peaks superimposed on the pressure trace are due to the 500 kHz mechanical resonance of the transducer. A rough extrapolation of the pressure trace indicates a value in excess of 52 kpsi at transducer failure. The complete decomposition of the sample under confinement could produce a maximum theoretical pressure of 239 kpsi within the 66 μl cell volume.

The IR absorption spectra in Figure 2 were obtained on a known sample weight between 0.505 inch diameter windows. The transmission (T = %T/100) and the sample density were used to calculate the Beer's law absorption coefficient. This value in combination with the laser pulse energy (E in joules), laser spot diameter (S in cm), and the sample heat capacity, Cp [20], was used to calculate the temperature rise, ΔK, within the sample region immediately behind the cell window. The complete formula is:

$$\Delta K = 0.396\ P\ E(\ln T)/\ [\ Cp\ W\ (\ln(1-P))\ S^2\ ] \qquad (1)$$

where W is the sample weight in grams used for the IR spectrum and P is the fraction of the laser pulse energy actually absorbed by the sample assuming nominal window reflection/transmission losses. Published investigations on HAN based propellants attribute the initial ignition reaction chemistry to the exothermic thermal decomposition of HAN[3,10,11] which occurs at 165 C. Equation (1) was used to obtain a ΔK of 140K which elevates the temperature to 165C from an initial temperature of 25C in the thin sample absorption region. This calculation

used an estimate for P of 0.9. The chosen laser spot diameter was 0.34 cm with T = 0.42(Figure 2) and the laser pulse energy was 0.59J. The variation of the temperature with laser pulse energy from Equation (1) is plotted in Figure 7. A series of laser pulse energies was used to experimentally establish the threshold needed for single pulse ignition/detonation and these energies are overlaid vertically on the calculated data. Ignition/detonation was experimentally observed at pulse energies $\geq$ 0.59J. The coincidence of the experimental data for the threshold laser value and the calculated line in Figure 7 required a value of 0.34 cm for the laser spot size in the calculation. The actual experimental spot size was 0.40 cm as measured roughly on bleached, thermally sensitive paper. These consistent experimental and calculated results support the following interpretations:

a) the laser pulse is strongly absorbed in a thin region of the sample,

b) resonant vibrational sample excitation due to absorption of the laser pulse is converted entirely to translational energy and rapid sample heating,

c) the heating of a thin layer of sample is sufficient to reach the known thermal decomposition temperature (165C) of HAN for a pulse energy of 0.59 J at 10.6 microns. This corresponds to an energy density of 4.7 J/cm^2.

The threshold laser pulse energy for ignition/detonation of 0.59 J represents a very small energy input of only 0.14 calories for the reliable, single pulse effect observed in the experiments using the cell in Figure 5a. Successful ignition/detonation was also achieved using the sample geometries in Figure 5b, c, and d. The smaller sample diameters required less pulse energy but a

constant energy density of 4.7 J/ cm^2 was required. This is consistent with Equation 2 and the thermal decomposition model where ΔK is proportional to pulse energy divided by the square of laser spot diameter. It is also interesting that HAN/HEHN mixtures containing added water were not successfully activated with single pulse energy densities of 4.7 J/cm^2. This is consistent with the published observations [8] that thermal decomposition within aqueous HAN mixtures only proceeds after significant energy is provided to drive off the water. Experiments on HEHN were uneventful with single laser pulses in the absence of oxidizer while no experiments on HAN itself were attempted since its absorption spectrum is nonresonant with the 10.6 micron laser.

Er- YAG Laser Experiments

The results for the single pulse ignition/detonation with the CO_2 laser at 10.6 μm suggest that other resonant laser wavelengths in the mid IR should be equally effective. Figure 8 depicts pressure versus time traces for 66 μl HAN/HEHN samples following the absorption of single 2.94 μm Er-YAG laser pulses of 544 mJ. The rapid oscillation at early time in Figure 8a has a < I μs period and it is most likely attributed to a reflected thermal shock between the cell entrance window and the face of the pressure transducer. In this case the BaF_2 cell entrance window failed quietly at 30 μs following the initial shock sequence. The failed window contained several radial cracks and most of the viscous sample appeared intact. In Figure 8b a violent ignition/detonation that began with a >23 kpsi pressure rise and ultimately the destruction of the window and pressure transducer after 30 μs is recorded. The traces in Figures 6b and 8b that were

initiated with single pulses of the CO_2 and Er-YAG lasers, respectively, show an initial pressure peak followed by a larger pressure rise. The Er-YAG result is elongated in time with respect to the CO_2 case but the temporal evolution in Figure 8b does not reflect the > 2 order of magnitude difference in the laser pulse widths in Figure 4b and c. This supports the interpretation that the sample requires the deposition of a threshold quantity of thermal energy to initiate the observed subsequent ignition event. A calculation using Equation (1) with 0.2 for T at 2.94 μm (Figure 2), 0.42 cm for S, 0.9 for P, and 0.50J for E gives the temperature elevation to165C that is required for HAN thermal decomposition. An experimental spot size of 0.40 cm and 0.52 J pulse energy was a typical ignition threshold at 2.94 μm.

The results at 2.94 μm are consistent with the assumptions inherent in Equation (1). The nearly equal threshold laser energy density of 4.1 and 4.7 J/cm^2 at 2.94 and 10.6 μm, respectively, supports the identical thermal decomposition model. An alternative photophysical mechanism of multiphoton IR photolysis is discounted since typical vibrational relaxation times in liquids are in the picosecond regime[21]. The laser pulse widths ranging from hundreds of nanoseconds at 10.6 μm to hundreds of microseconds at 2.94 μm would not allow the necessary vibrational ladder climbing required for multiphoton IR photochemistry with such rapid V → T relaxation. The combined infrared results indicate that the strongly absorbing sample requires sufficient cumulative energy from the laser pulse to reach a threshold temperature for HAN thermal

decomposition. Further reaction chemistry then follows under conditions of self pressurization.

Excimer Laser Experiments

The HAN-HEHN UV absorption spectrum in Figure 1 indicates the positions of the two resonant excimer wavelengths. Attempts to ignite samples with single and multiple 115 mJ pulses at 193 nm and 250 mJ at 248 nm using the cell design in Figure 5a were unsuccessful. In general S1-UV grade fused silica windows from 1/16 to 3/16 inch thickness were cracked and a portion of the sample typically became frothy.

Three pathways exist for the disposition of UV excitation within the sample: photolysis, radiative relaxation (fluorescence/phosphorescence), and nonradiative excited state quenching to yield heat. All three pathways are possible during these experiments, although no attempts were made to detect UV/VIS emission. It is, therefore, possible that pulse energies in excess of those available are required to achieve the same temperature rise with UV photons that leads to HAN thermal decomposition and further reaction as in the mid IR. Photolysis is likely at 193 nm but the photolytic specificity leads to either unproductive and/or insufficient fragmentation with regard to ignition initiation.

Conclusions

a) Despite a 2 order of magnitude difference in laser power density between experiments at 2.9 and 10.6 μm both mid IR lasers gave rise to single pulse ignition/detonation by simple vibrational heating at comparable energy densities.

This vibrational heating is consistent with HAN thermal decomposition in a thin sample region behind the cell entrance window and subsequent ignition/detonation following a combined chemical induction and thermal conduction period on the microsecond timescale. The nearly equal threshold laser energy density of 4.1 and 4.7 J/cm^2 at 2.94 and 10.6 μm, respectively, supports an identical HAN thermal decomposition model at these wavelengths. As long as efficient V → T energy transfer and ensuing sample heating occurs the identity of the sample absorption resonance with the laser is not critical. A focused IR laser spot (< 4 mm) could reduce the energy needed for single pulse ignition/detonation below the 0.5 J range. A lower limit determination would allow projections for laser miniaturization.

b) The resonant mid IR lasers are convenient means to provide the rapid propellant heating that leads to ignition/detonation under confinement. The miniaturization potential of the solid state laser at 2.94 μm is especially attractive for practical applications for the HAN/HEHN mixture but any resonant mid IR wavelength should also be effective. This study can be framed within a more general overview of ignition/detonation phenomena contained in the paper by Ronney (2004)

c) The experiments conducted with resonant 193 and 248 nm wavelengths in the UV did not achieve ignition/detonation at the pulse energy limits of 115 mJ and 250 mJ, respectively. The resonant UV wavelengths excited electronic transitions that yielded some photolysis as well as nonradiative relaxation to

thermal heating and perhaps some undetected fluorescence. A compact, suitably high energy laser source in the UV is not available as in the IR.

d) Computational modeling that provides estimates of the conditions (minimum pulse energy and spot size; minimum self pressurization vs. sample size) required to progress to other IL materials and sample formats is in progress.

References

1. Klingenberg, G., Knapton,J.D., Morrison, W.F.,and Wren,G.P. (1998) *Liquid Propellant Gun Technology*, American Institute of Aeronautics and Astronautics, Inc., Reston, VA.

2. Farshchi, M., Vaezi, V., and Shaw, B.D. (2002) Studies of HAN-based monopropellant droplet combustion, *Combust. Sci. and Tech*., **174**, 71.

3.Carleton, F.B., Klein, N., Krallis, K., and Weinberg, F.J. (1992) Initiating reaction in liquid propellants by focused laser beams, *Combust. Sci. and Tech.*, **88**, 33.

4. Call, C. and Deevi, S.C. (1997) Combustion and microexplosion of Han-based liquid gun propellants at elevated pressures, *J. Propulsion*, **13**, 448.

5. R. A. Beyer (1996), *Laser Ignition of Liquid Gun Propellant XM46*, Report ARL-TR-1058, Army Research Laboratory, Aberdeen Proving ground, MD, USA.

6. Beyer, R.A. and Reeves, G.P. (1997) *Laser Ignition of Liquid Gun Propellant XM46: Ignition of Larger Volumes,* Report ARL-TR-1292, Army Research Laboratory, Aberdeen Proving ground, MD, USA.

7. R.A. Beyer (1994) *Method of confinement of propellants for ignition*, US Patent 5,359,919 , The United States of America, Washington, D.C., USA.

8. Lee, Y. J. and Litzinger, T.A. (1999) Combustion chemistry of HAN, TEAN, and XM46, *Combust. Sci. and Tech.*, **141**, 19.

9. Chang, Y.P., Boyer, E., and Kuo, K.K. (2000) Combustion Behavior and Flame Structure of XM46 Liquid Propellant, AIAA 2000-0706, 2000, Reno, 10-13 January.

10. Amariei, D., Courtheoux, L., Rossignol, S., Batonneau, Y., Kappenstein, C., Ford, M. and Pillet, N. (2005) Influence of the fuel on the thermal and catalytic decompositions of ionic liquid monopropellants, AIAA 2005-3980, Tucson, 10-13 July.

11. Wei, C., Rogers, W.J., and Mannan,, M.S. (2006) Detection of autocatalytic decomposition behavior of energetic materials using APTAC, *J. Thermal Analysis and Calorimetry* **, 83**, 125.

12. Sofue, T. and Iwama, A. (1979) Ignition of composite propellant at subatmospheric pressure by means of carbon dioxide laser, *Propellants and Explosives*, **4**, 98.

13. de Yong, L and Lui, F. (1998) Radiative ignition of pyrotechnics: Effect of wavelength on ignition threshold, *Propellants, Explosives, Pyrotechnics* , **23**, 328.

14. Ahmad, S.R. and Russell, D.A. (2001) Studies into laser ignition of unconfined propellants, *Propellants, Explosives, Pyrotechnics* , **26**, 235.

15. Gillard, Ph. and Roux, M. (1997) Ignition of Pyrotechnic Mixture by Means of a Laser Diode. Part 1; Numerical Modeling, *Propellants, Explosives, Pyrotechnics*, **22**, 256.

16. Ding, D. (2006) A Study on the ignition of boron/potassium nitrate mixture, *Sci. Tech. Energetic Materials*, **67**, 23.

17. Koizumi, H., Nakano, M., Inoue, T., Watanabe, M., Komurasaki, K., and Arakawa, Y. (2006) Study on laser ignition of boron/potassium nitrate in vacuum, *Sci. Tech. Energetic Materials* , **67**, 193.

18. Wucherer, E.J., Christofferson, S., and Reed, B. (2000) Assessment of High Performance HAN-Monopropellants, AIAA 2000-3872, Huntsville, 16-19 July.

19. Schmidt, E. (2001) *Hydrazine and Its Derivatives*, Wiley-Interscience, New York, Volume 1. 2nd ed. Chapter 2.

20. McKay, M. (2008) AFRL Edwards Air Force Base, Private Communication.

21. Oxtoby, D.W. (1981) Vibrational relaxation in liquids, *Ann. Rev. Phys. Chem.*, **32**, 77.

22. Ronney, P.D. (2004) Laser versus conventional ignition of flames, *Opt. Eng.*, **33**, 510.

Acknowledgements

This work was performed at Edwards AFB under a Cooperative Research and Development Agreement (USAF CRADA 07-283-PR-01) between the Air Force Research Laboratory and Northrop Grumman Space Technology (NGST). Financial and facilities support from AFOSR, EAFB, and the Technology and Emerging Systems Division of NGST is gratefully acknowledged.

Figure Captions

1. Ultraviolet absorption spectrum of HAN-HEHN mixture with coincident excimer wavelengths highlighted. Expanded view near 248 nm in inset.

2. Infrared absorption spectrum of HAN-HEHN mixture in resonance regions of Er-YAG (2.94 μm) and CO_2 laser (10.6 μm).

3. Time-resolved wavelength distribution of multiline CO_2 laser pulse. 5 ns per temporal slice.

4. Temporal profiles of a) excimer laser, b) CO_2 laser, and c) Er-YAG laser pulses.

5. Sample cell geometries with various volumes: a) 66 μl, b) 31 μl, c) 19μl, and d) 11 μl. The laser pulse energy per unit area was kept constant with additional apertures.

6. Temporal profiles of ignition/detonation pressure and optical emission following single CO_2 laser pulses. Ordinate scale for both pressure traces is 3908 psi/division; laser pulse and optical emission are uncalibrated transducer voltages.

7. Calculated laser pulse energy-temperature dependence (squares) with superimposed experimental ignition energy (triangles) threshold.

8. Temporal profiles of a) pressure rise for nondetonating event and b) ignition/detonation pressure following single Er-YAG laser pulses.

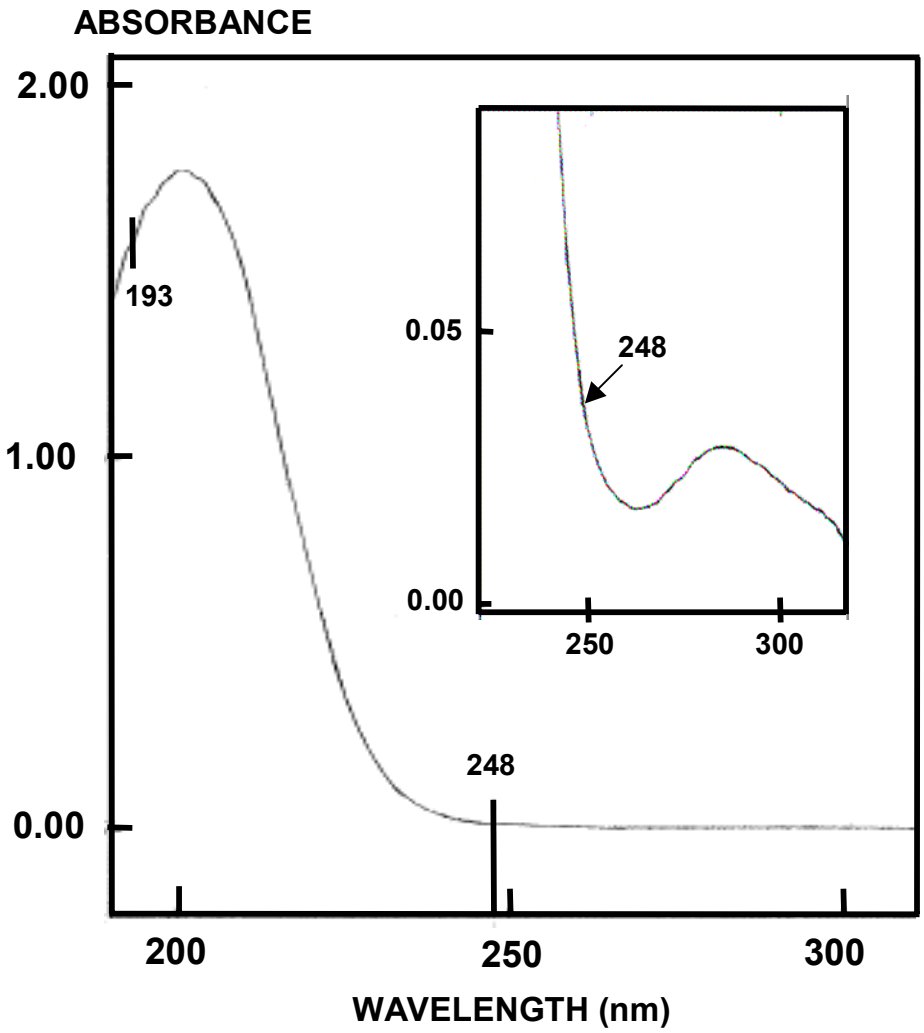
ABSORBANCE
2.00
1.00
0.00
193
248
200
250
300
WAVELENGTH (nm)
0.05
0.00
248
250
300

Fig. 1

Fig. 2

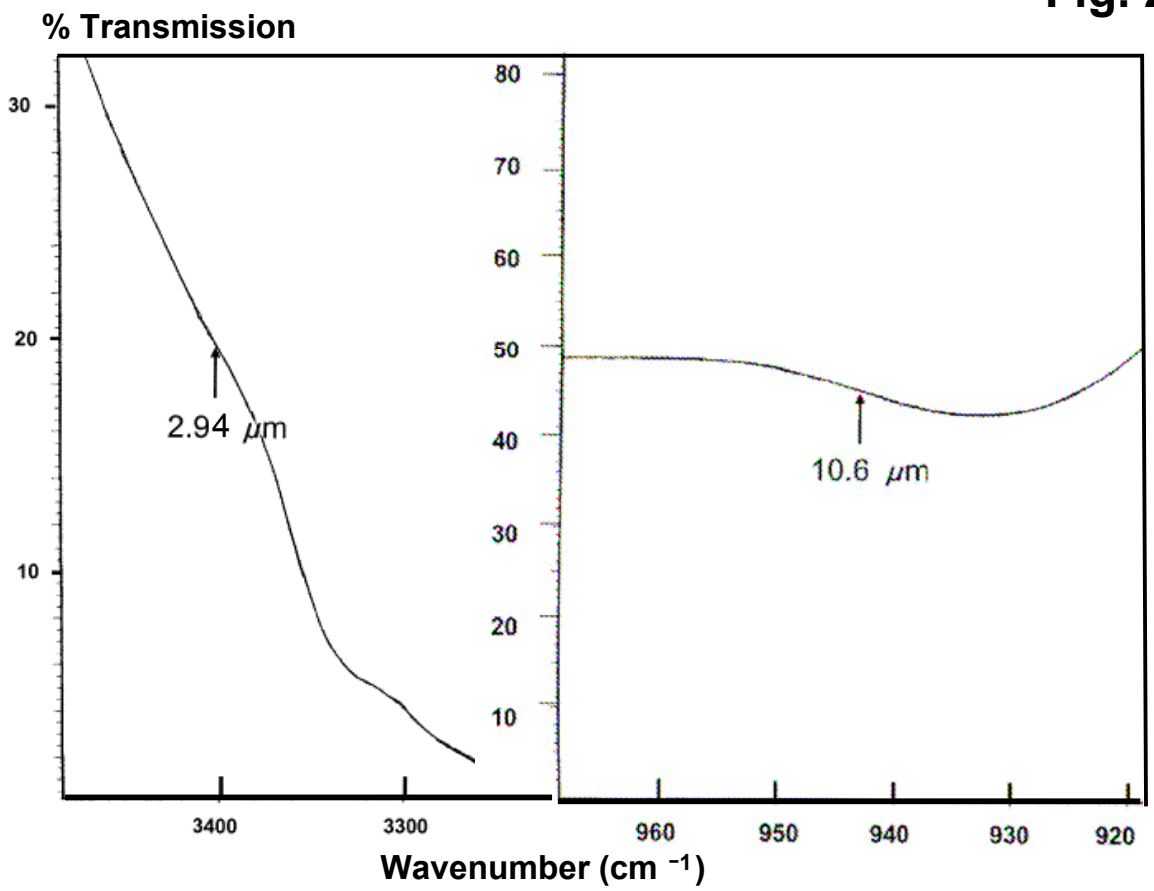
% Transmission
30
20
10
80
70
60
50
40
30
20
10
2.94 μm
10.6 μm
3400
3300
960
950
940
930
920
Wavenumber (cm −1)

Fig. 3

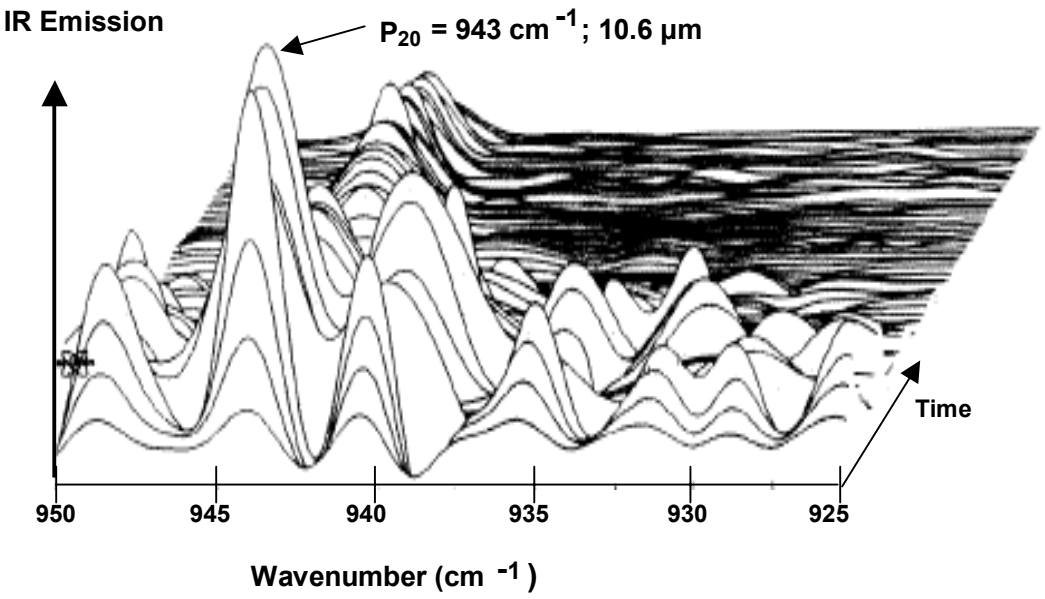
IR Emission
P20 = 943 cm -1; 10.6 µm
Time
950
945
940
935
930
925
Wavenumber (cm -1)

Fig. 4

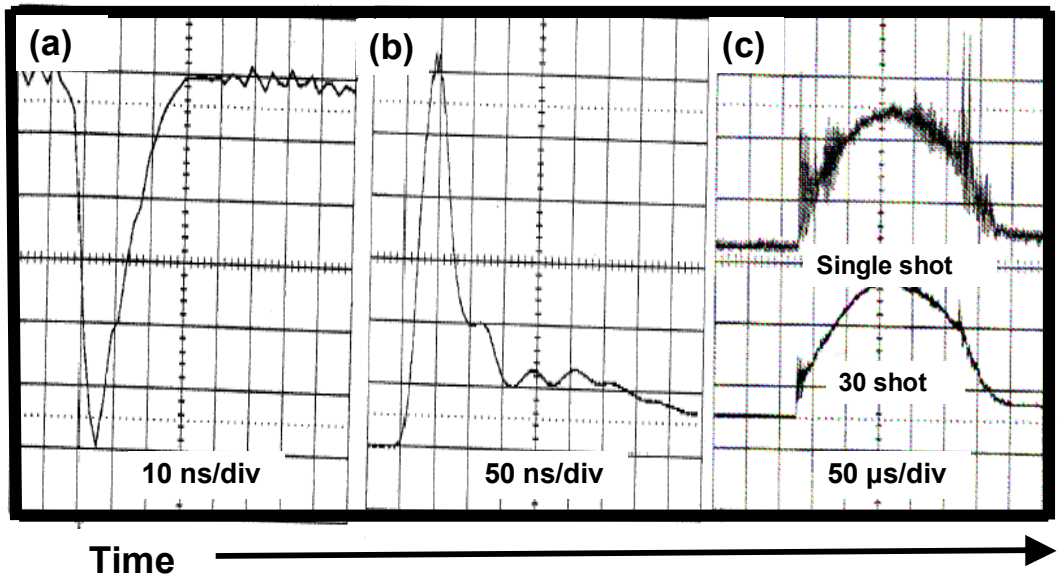

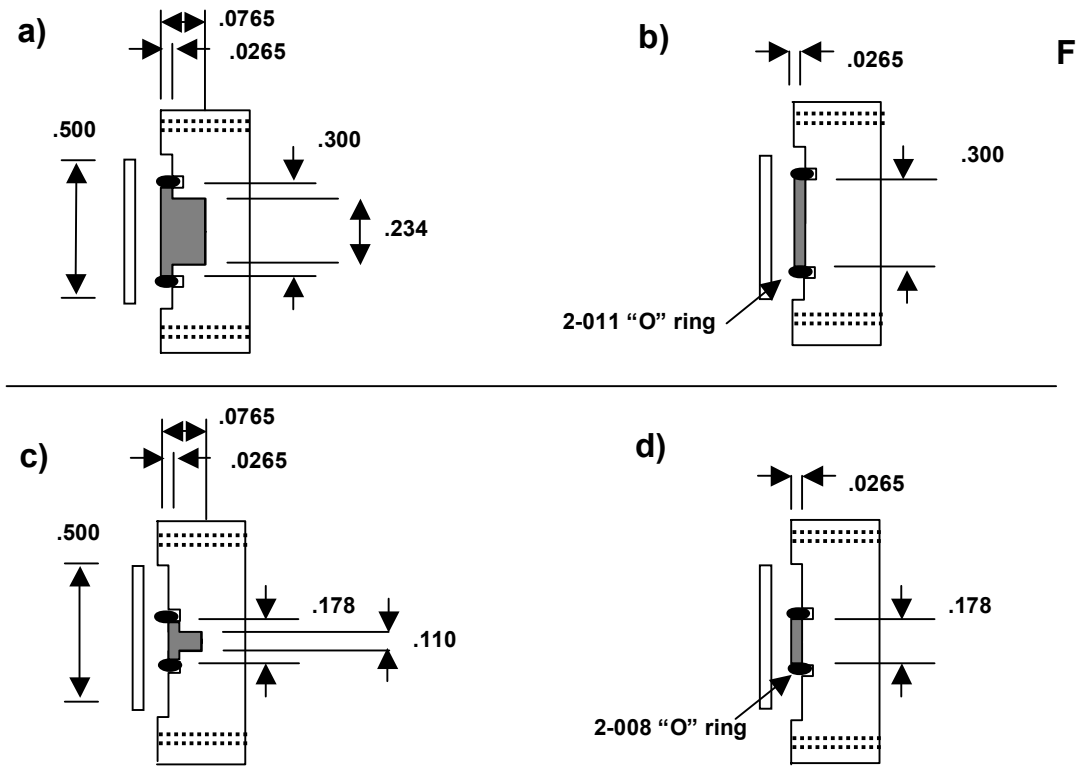
a)
.0765
.0265
.500
.300
.234
b)
.0265
.300
2-011 "O" ring
c)
.0765
.0265
.500
.178
.110
d)
.0265
.178
2-008 "O" ring

Fig.5

Fig. 6

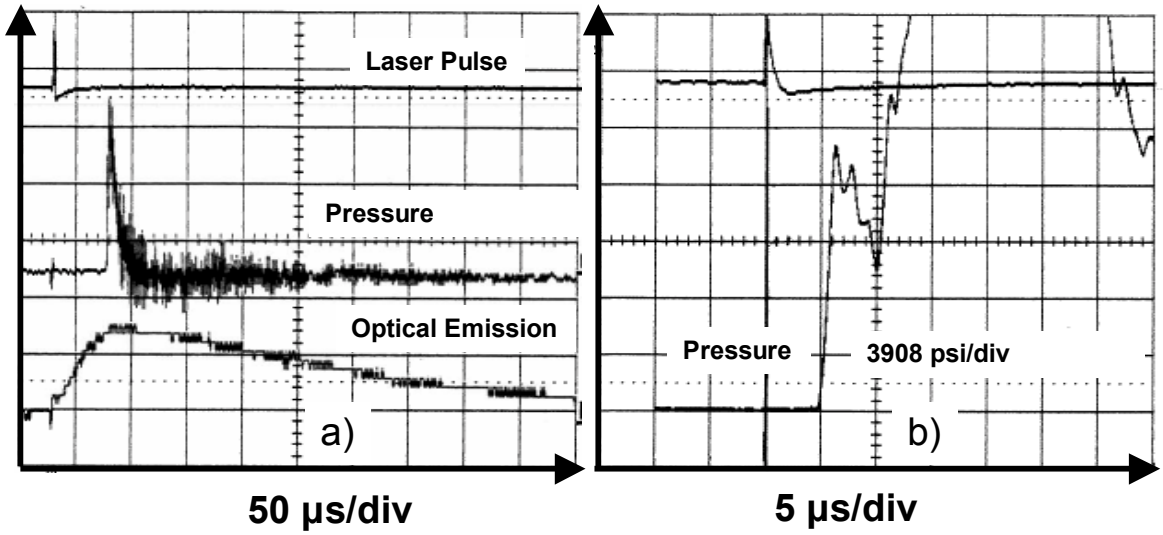
Laser Pulse
Pressure
Optical Emission
a)
Pressure
3908 psi/div
b)
50 µs/div
5 µs/div

Fig. 7

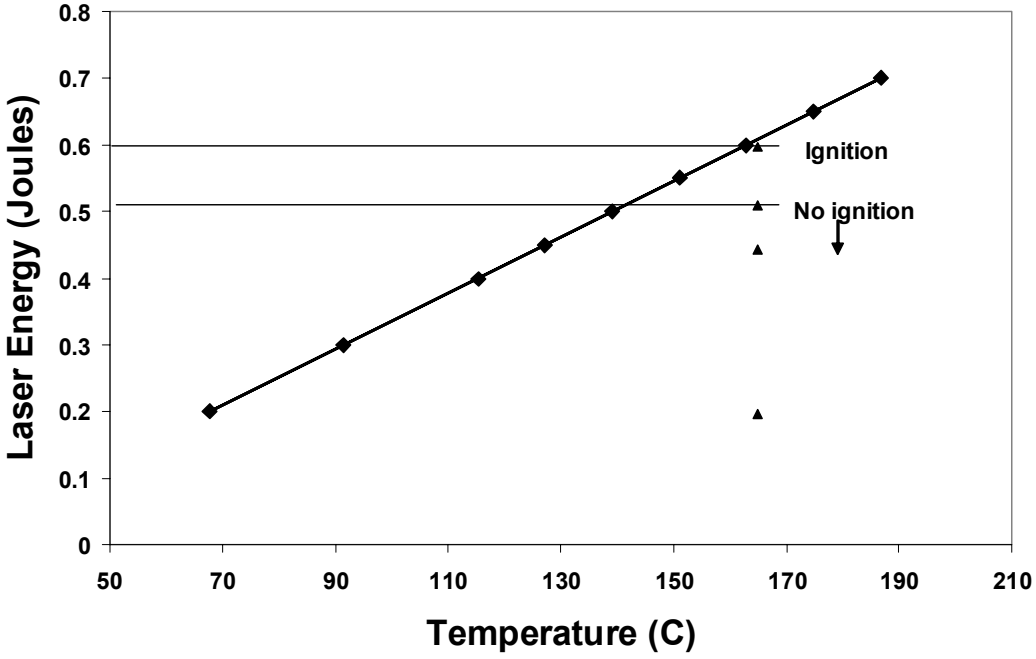
Laser Energy (Joules)
0.8
0.7
0.6
0.5
0.4
0.3
0.2
0.1
0
50
70
90
110
130
150
170
190
210
Temperature (C)
Ignition
No ignition

Fig. 8